

**Outdoor Sunlight Driven Scalable Water-Gas Shift Reaction Through Novel
Photothermal Device Supported $\text{CuO}_x/\text{ZnO}/\text{Al}_2\text{O}_3$ Nanosheets with $192 \text{ mmol g}^{-1} \text{ h}^{-1}$ of
Hydrogen Generation Rate**

Chengcheng Shi,^{‡a} Dachao Yuan,^{‡b} Luping Ma,^b Yaguang Li,^{*a} Yangfan Lu,^c Linjie Gao,^{*a}
Xingyuan San,^a Shufang Wang,^{*a} Guangsheng Fu^a

[a] Hebei Key Lab of Optic-electronic Information and Materials, The College of Physics
Science and Technology, Institute of Life Science and Green Development, Hebei University,
Baoding, 071002, China.

[b] College of Mechanical and Electrical Engineering, Hebei Agricultural University,
Baoding 071001, P. R. China

[c] School of Materials Science and Engineering, State Key Laboratory of Silicon Materials,
Zhejiang University, Hangzhou 310027, P. R. China.

Correspondence and requests for materials should be addressed to Y.G. Li
(yaguang_1987@126.com), L.J. Gao (LinjieGao@hotmail.com), S.F. Wang
(sfwang@hbu.edu.cn).

[‡] These authors contributed equally.

Experimental Section

1.1 Chemicals

The Cr film based photothermal device was provided by Hebei scientist research experimental and equipment trade Co., Ltd. $\text{Zn}(\text{NO}_3)_2 \cdot 6\text{H}_2\text{O}$ (AR, 99%), $\text{Al}(\text{NO}_3)_3 \cdot 9\text{H}_2\text{O}$ (AR, 99%), Na_2CO_3 (AR, 99%) and borax (AR, 99%) were purchased from Fuchen chemical industry. $\text{Cu}(\text{NO}_3)_2$ (AR, 99%) was bought from Macklin Co., Ltd. All chemicals were used without any further treatment.

1.2 Catalysts preparation

The catalysts were prepared by co-precipitation method. Typically, stoichiometric 37.512g $\text{Cu}(\text{NO}_3)_2$, 29.749g $\text{Zn}(\text{NO}_3)_2 \cdot 6\text{H}_2\text{O}$ and 12.504g $\text{Al}(\text{NO}_3)_3 \cdot 9\text{H}_2\text{O}$ were dissolved into 200 ml deionized water, after stirring for 1 h, the resulted solution and NaCO_3 aqueous solution (0.2 mol/L; 1000 ml) was added dropwise into 100 ml borax buffer solution (3.81 g with 100 ml deionized water), and stirred at 65 °C for 1 h. After hold at 65 °C for 4 h and aging for 7 h, the resulting precipitate was washed several times by deionized water, and then fast-frozen by liquid nitrogen. The frozen cube was freeze-dried at -55 °C and then calcinated in air at 400 °C for 6 h to obtain Cu-Zn-Al based oxides. Finally, the products were reduced in 10% H_2/Ar at 300 °C for 10 h, and 2D CuZnAl catalysts were formed during this process.

For comparison, we synthesized another CuZnAl sample reproduced the above processes and the only difference was that using aqueous solution to replace the borax buffer solution. The sample was named as CuZnAl.

1.3 Characterizations of Catalysts

X-ray diffraction (XRD) patterns of prepared samples were collected by a Bede D1 system operated at 20 kV and 30 ma with Cu $K\alpha$ radiation ($\lambda=1.5406 \text{ \AA}$). For microstructure observation, field emission scanning electron microscopy (FE-SEM, FEI Nova NanoSEM450) and transmission electron microscope (TEM, JEOL F200 + ARM 200 F) was used. The optical properties were investigated by a Hitachi Limited U4100 UV-Vis spectrophotometer

and a FTIR spectrometer (Bruker, VERTEX 70 FT-IR). The BET surface areas were obtained using a Micromeritics Tristar 3020 system. The XPS spectra were recorded on a Thermo ESCALAB-250 spectrometer using a monochromatic Al K α radiation source (1486.6 eV). The binding energies determined by XPS were corrected by referencing the adventitious carbon peak (284.6 eV) for each sample. The steady-state PL measurements were performed on a FLS920 fluorescence spectrophotometer (Edinburgh Instruments).

1.4 Thermal catalytic test

The thermal WGS catalytic activity of 2D CuZnAl and commercial CuZnAl was tested by the fixed-bed reactor (XM190708-007, DALIAN ZHONGJIARUILIN LIQUID TECHNOLOGY CO., LTD) in continuous flow form. Typically, 10 mg catalyst was placed in a quartz flow reactor. The feed gas composition was (vol.) 4 % CO and 6 % H₂O balanced with Ar (the gas flow rate of CO+Ar is 60 sccm). The reaction products were tested by gas chromatograph (GC) 7890A equipped with FID and TCD detector.

1.5 Sunlight-driven WGS reaction

The laboratory light source we used for photothermal test is a customized product (HP-2-4000, provided by Hebei scientist research experimental and equipment trade Co., Ltd), which has uniform irradiation area of 0.8 m * 0.3 m with 10 % light intensity fluctuation. And the light emission spectrum was shown in Figure S9, which was similar to AM 1.5G. The light intensity was measured by an irradiance meter (I400).

1.5.1 Laboratory sunlight-driven WGS reaction

10 mg of prepared catalysts were loaded in a quartz tube or photothermal device (irradiation area 0.56 cm²) irradiated by HP-2-4000. The irradiation intensity was tuned from 0.1 kW m⁻² to 1 kW m⁻² and 6 kW m⁻². The feed gas composition was (vol.) 4 % CO and 6 % H₂O balanced with Ar (the gas flow rate of CO+Ar is 60 sccm). The reaction products were tested by gas chromatograph (GC) 7890A equipped with FID and TCD detector.

1. The hydrogen generation rate for per gram of catalyst (δ , $\text{mmol g}_{\text{cat}}^{-1} \text{h}^{-1}$) shown in Figure 3b was calculated as follows:

$$\delta (\text{mmol g}_{\text{cat}}^{-1} \text{h}^{-1}) = (1000 * K * L * 60 / 22.4) / G \quad (1)$$

K was the hydrogen concentration detected by GC, L was the gas flow rate, G was the weight of catalysts of 0.01 g.

2. The plate form hydrogen generation rate (η , $\text{L m}^{-2} \text{h}^{-1}$) shown in Figure 3c was calculated as follows:

$$\eta (\text{L m}^{-2} \text{h}^{-1}) = K * L * 60 / S \quad (2)$$

K was the hydrogen concentration detected by GC, L was the gas flow rate, S was the irradiated area of catalysts of 0.56 cm^2 .

3. The efficiency of light-to-combustion energy storage (δ) was calculated by the following formula:

$$\delta = [r(\text{H}_2) * (\Delta H(\text{H}_2) - \Delta H(\text{CO}))] / P * 100\%$$

$r(\text{H}_2)$: generation rate of H_2 (1.90 mmol h^{-1});

$\Delta H(\text{H}_2)$: combustion heat of H_2 , $285.8 \text{ kJ mol}^{-1}$;

$\Delta H(\text{CO})$: combustion heat of CO , $282.8 \text{ kJ mol}^{-1}$;

P : power of light irradiation (0.201 KJ h^{-1}).

The efficiency is about 2.86 %.

1.5.2 Outdoor sunlight-driven thermal WGS reaction

Since the sunlight intensity was too weak in the morning and evening, we added reflectors with 4.2 m^2 of irradiated area to make the photothermal device able to work in all day time. The install of parabolic reflector was based on the ecliptic plane to make sunlight focus on new photothermal conversion tube. 1 kg of prepared catalyst was loaded in the photothermal device and only the outdoor sunlight was used as the light source. A hand hold multifunctional complex gas analyzer (JK90-M7) was used to test the reaction gases. The feeding gas was pure CO with $2 \text{ m}^3 \text{ h}^{-1}$ flow rate and water was supplied by water tank with

the rate of 3 kg h⁻¹. The exhaust entered the compressor to make CO₂ pressurized into dry ice and the dry ice was used as the fertilizer of the greenhouse of Hebei Agricultural University.

1. The light intensity was detected by an irradiance meter (I400).
2. The temperatures of catalysts were determined by a platinum resistance thermometer (M363886).
3. The total H₂ production amount (η) was calculated by the following formula:

$$\eta \text{ (m}^3\text{)} = K * L \quad (1)$$

K (=0.734 m³ h⁻¹) was the average H₂ production rate from 8:00 to 17:00 (shown in Figure 4d), L was the total time (9 h).

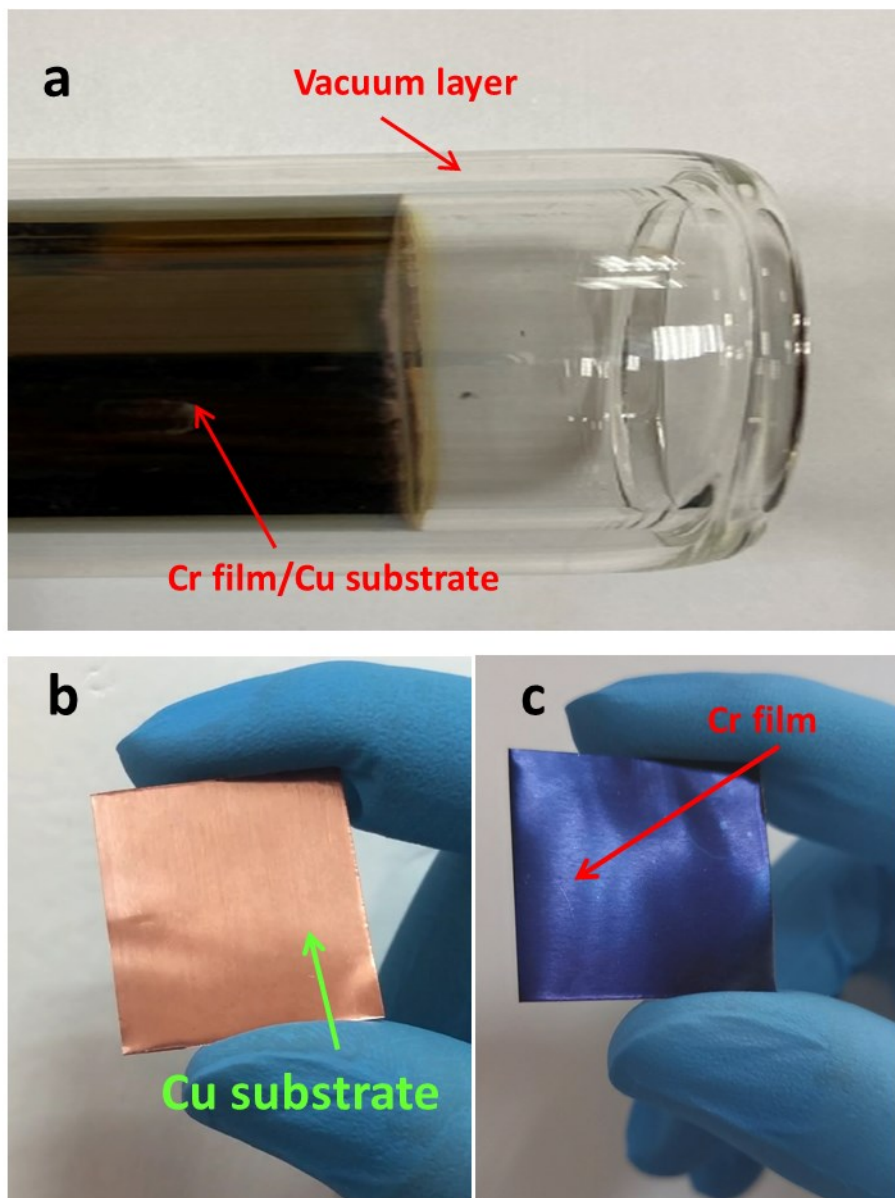


Figure S1. (a) is the photograph of photothermal device. (b, c) Photograph of Cu substrate and Cr film, respectively.

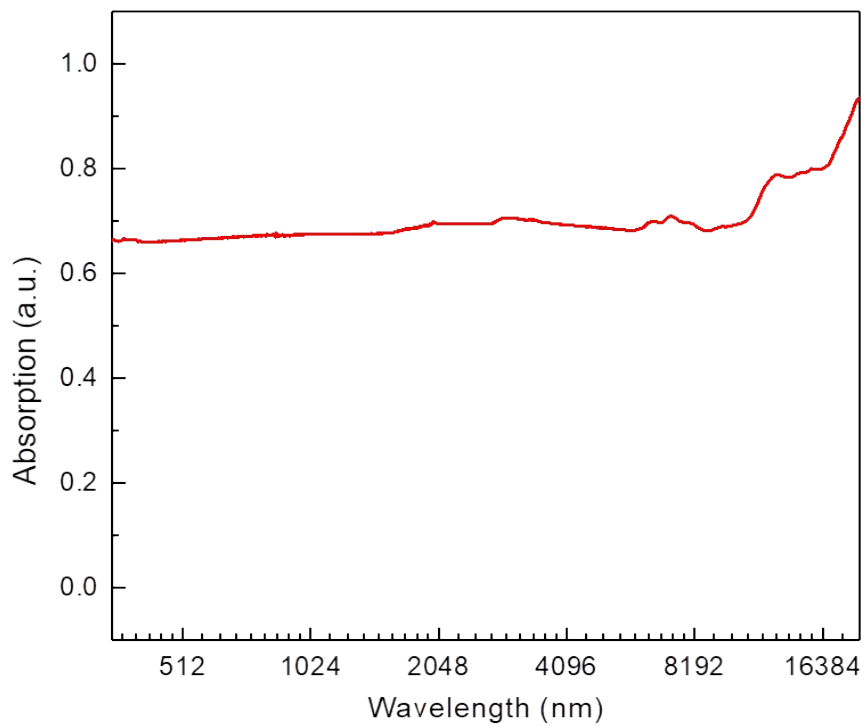


Figure S2. Normalized light absorption spectrum of 2D CuZnAl ranging from 0.4 to 20 μm .

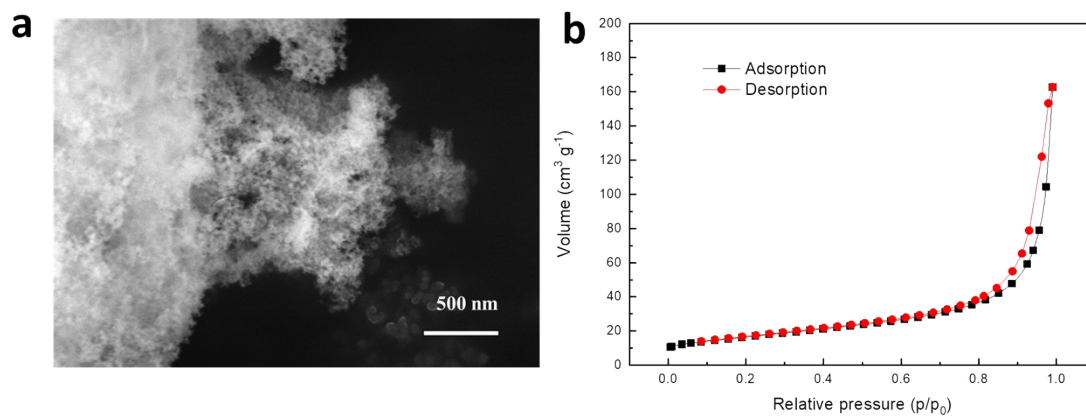


Figure S3. (a)SEM image, (b) Nitrogen adsorption and desorption isotherm of the CuZnAl.

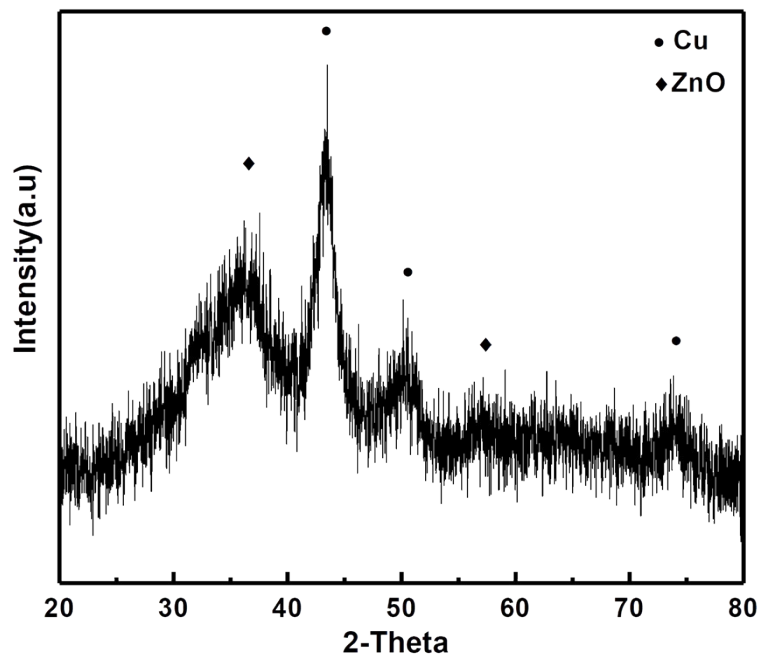


Figure S4. XRD pattern of the 2D CuZnAl.

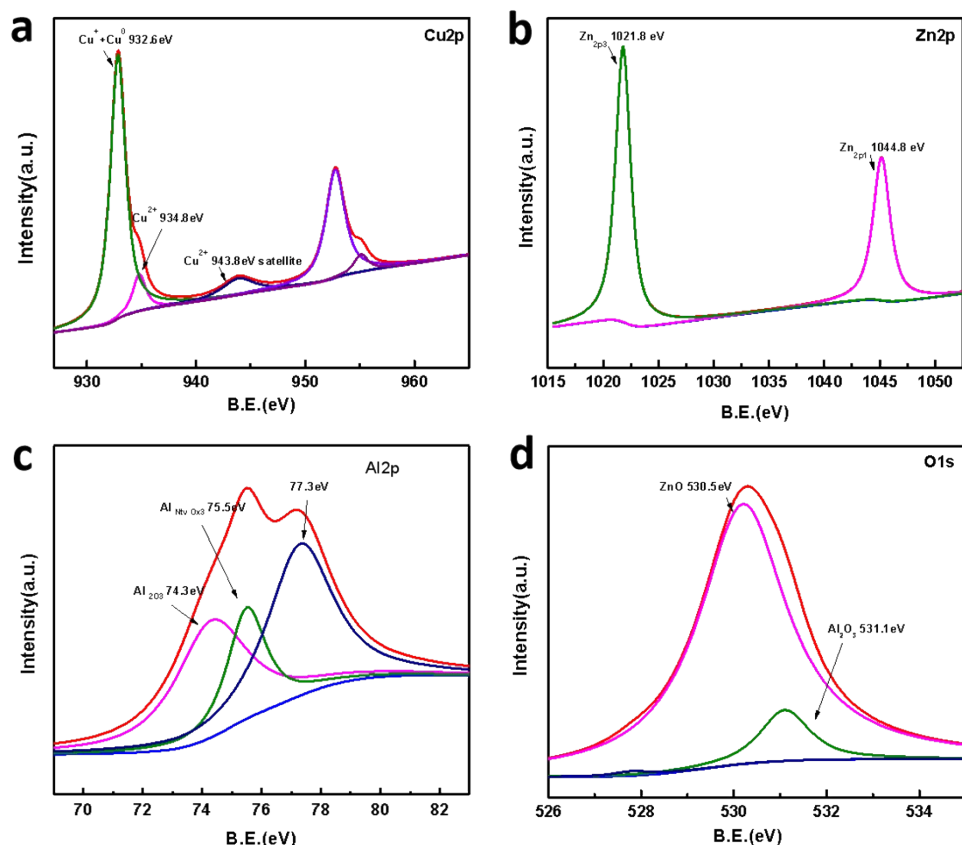


Figure S5. (a, b, c, d) Cu 2p, Zn 2p, Al 2p, O1s XPS of the 2D CuZnAl.

The phase composition and chemical states of 2D CuZnAl are determined by X-ray diffraction (XRD) and X-ray photoelectron spectroscopy (XPS). According to the XRD pattern in Figure S4, diffraction peaks belong to ZnO and metallic Cu can be observed,^{2,4} while the peak assigned to Al₂O₃ is not detectable either because of its amorphous nature.⁵ XPS measurements reveal that both metallic Cu and a small amount of Cu²⁺ are co-existed in this sample (Figure S5).⁶ The O 1s peaks are mainly dominated by the contribution from ZnO and Al₂O₃.^{7, 8} Therefore, the sample is composed by CuO_x, ZnO and Al₂O₃.

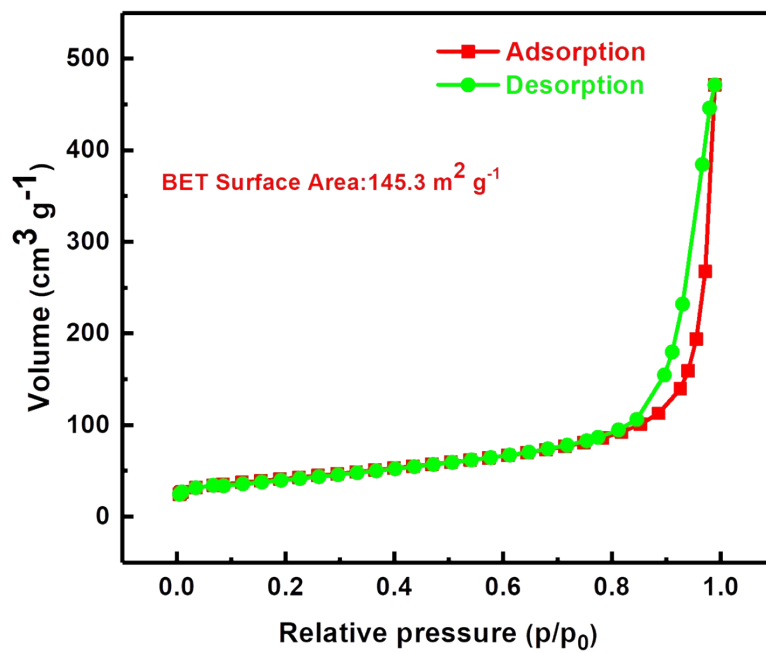


Figure S6. Nitrogen adsorption and desorption isotherm of the 2D CuZnAl.

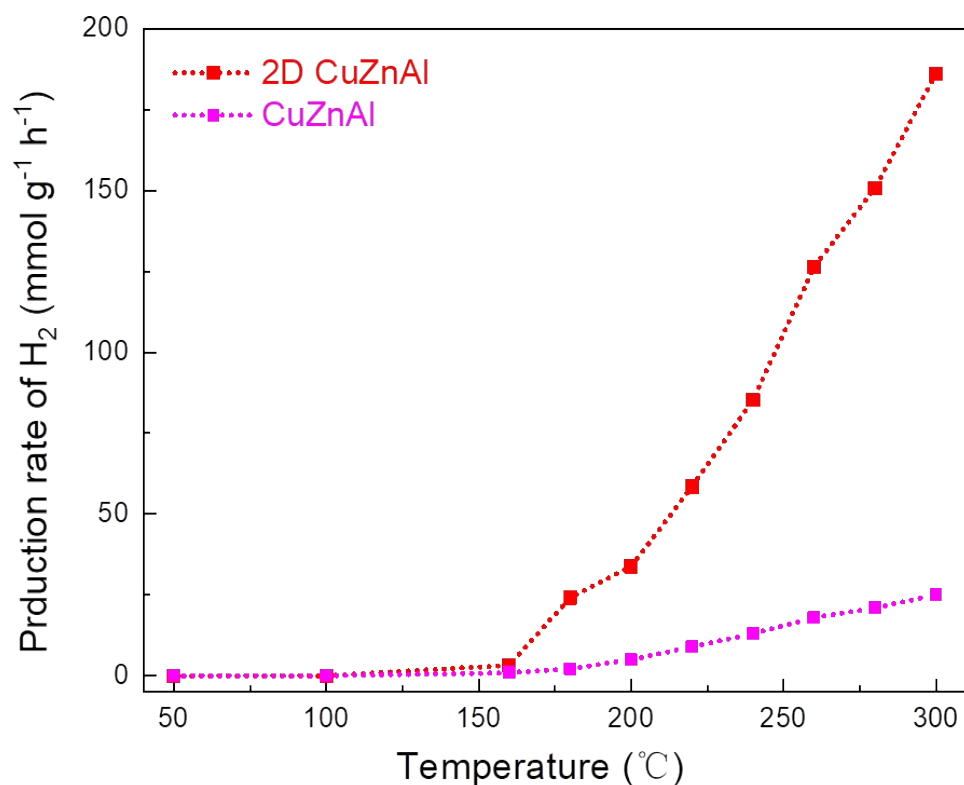


Figure S7. Hydrogen production rate from thermal WGS reaction of the 2D CuZnAl and CuZnAl at different temperature.

We tested the thermal WGS performance of 2D CuZnAl in comparison with CuZnAl. Compared with CuZnAl, 2D CuZnAl showed a better WGS performance (Figure S7). At the temperature of 160 °C, the signal of hydrogen can be detected from 2D CuZnAl, while no hydrogen was generated over CuZnAl. As the temperature reached to 300 °C, the hydrogen generation rate was 188.69 mmol g⁻¹ h⁻¹ for 2D CuZnAl, 6 times higher than that of CuZnAl (Figure S7).

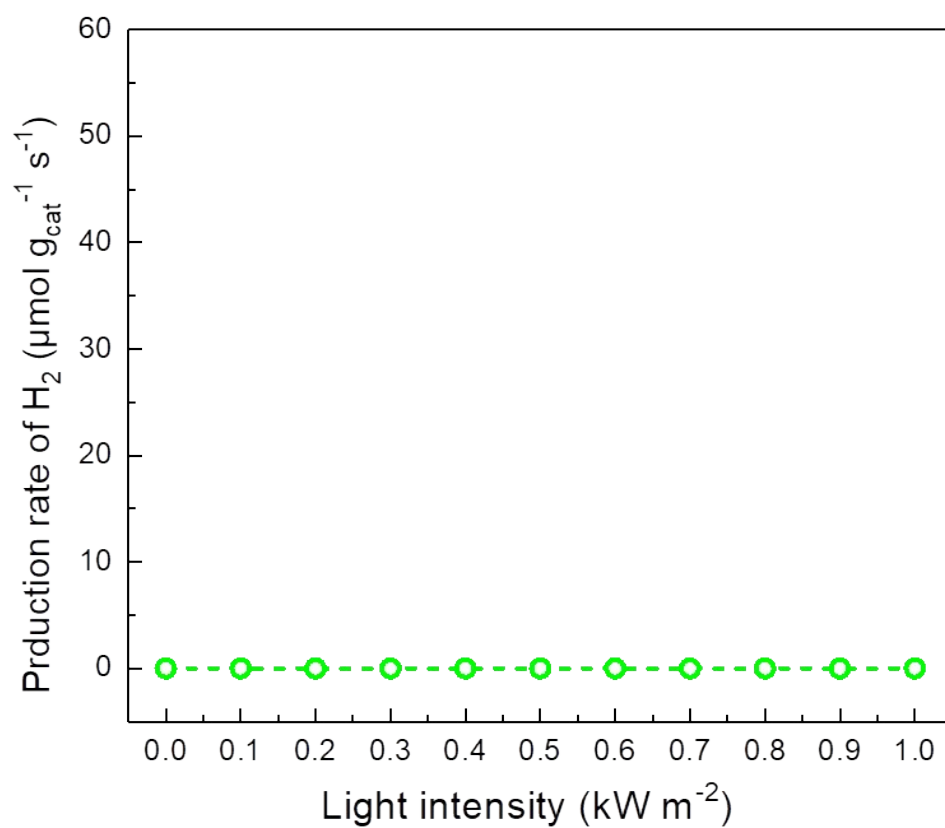


Figure S8. The H₂ generation rate from WGS reaction of 2D CuZnAl under different intensities of solar irradiation.

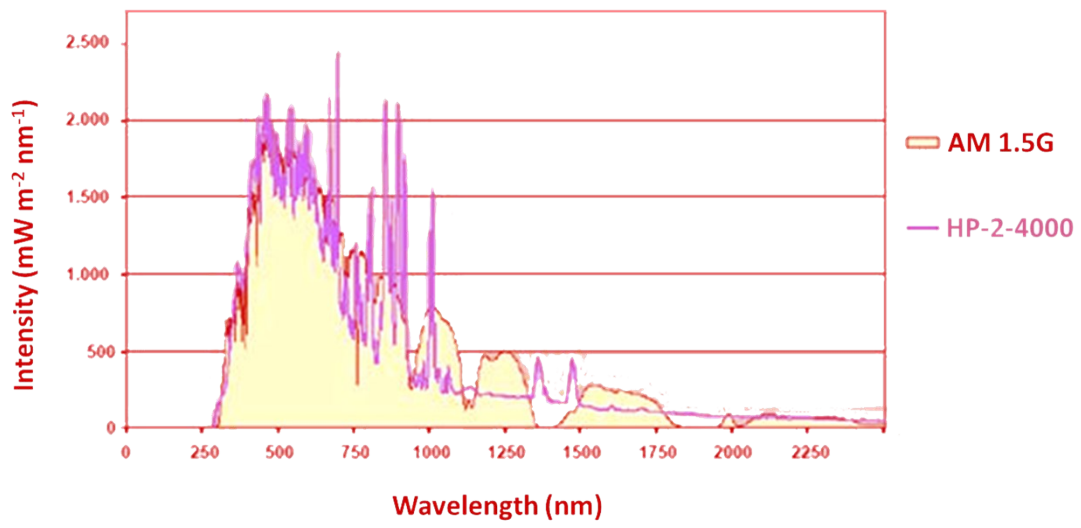


Figure S9. The light spectrum of HP-2-4000.

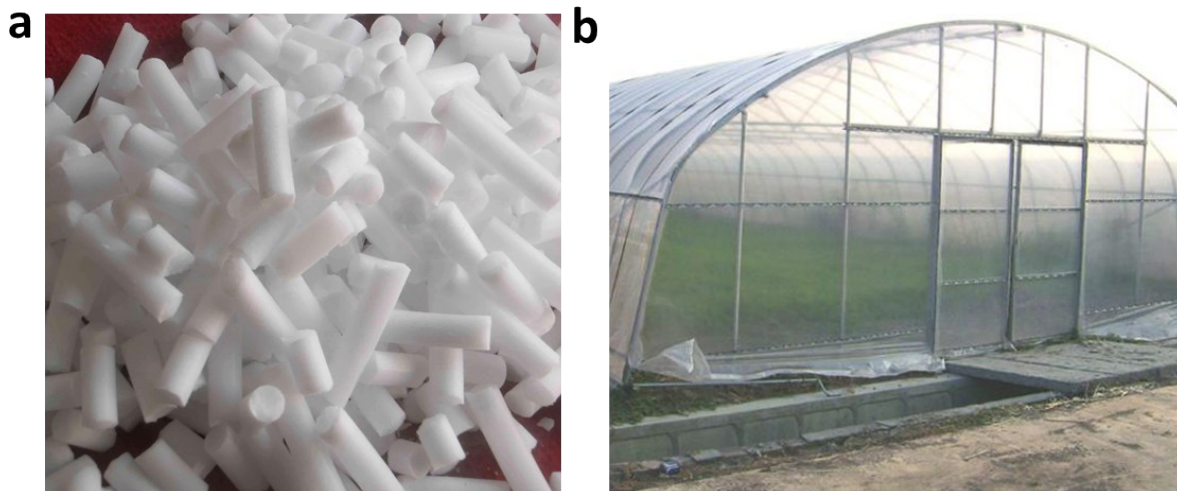


Figure S10. (a) The dry ice produced from the exhausted CO_2 of outdoor sunlight driven thermal WGS reaction. (b) The green house of Hebei Agricultural University.

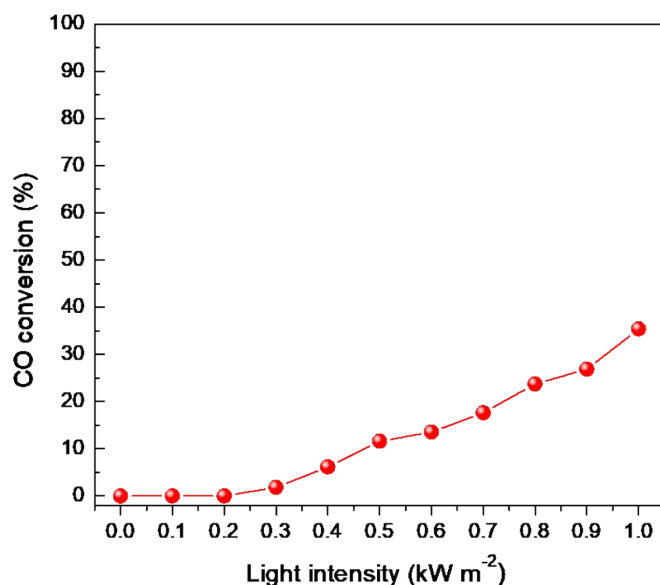


Figure S11. The curve of CO conversion from WGS reaction of 2D CuZnAl supported by new photothermal device, under different intensities of solar irradiation.

References

1. L. K. Zhao, Y. H. Qi, L. Z. Song, S. B. Ning, S. X. Ouyang, H. Xu and J. H. Ye, *Angew. Chem. Int. Ed.*, 2019, **58**, 7708-7712.
2. M. Hou, L. Ma, H. Ma and M. Yue, *J. Mater. Sci.*, 2017, **53**, 1065-1075.
3. Y. Tanaka, T. Utaka, R. Kikuchi, K. Sasaki and K. Eguchi, *Applied Catalysis A: General*, 2003, **238**, 11-18.
4. J. L. Santos, T. R. Reina, S. Ivanova, M. A. Centeno and J. A. Odriozola, *Applied Catalysis B: Environmental*, 2017, **201**, 310-317.
5. O. A. Bulavchenko, Z. S. Vinokurov, A. A. Saraev, A. M. Tsapina, A. L. Trigub, E. Y. Gerasimov, A. Y. Gladky, A. V. Fedorov, V. A. Yakovlev and V. V. Kaichev, *Inorg. Chem.*, 2019, **58**, 4842-4850.
6. C. He, Y. Yu, L. Yue, N. Qiao, J. Li, Q. Shen, W. Yu, J. Chen and Z. Hao, *Applied Catalysis B: Environmental*, 2014, **147**, 155-166.
7. S. D. Jones, L. M. Neal and H. E. Hagelin-Weaver, *Applied Catalysis B Environmental*, 2008, **84**, 631-642.
8. F. Raimondi, K. Geissler, J. Wambach and A. Wokaun, *Applied Surface Science*, 2002, **189**, 59-71.